Low Band Gap and Ionic Bonding with Charge Transfer Threshold in the Polymeric Lithium Fulleride Li_4C_{60}

Roberto Macovez,[†] Rebecca Savage,[†,‡] Luc Venema,[†] Joachim Schiessling,[‡] Katalin Kamarás,[§] and Petra Rudolf*[,†]

Zernike Institute for Advanced Materials, University of Groningen, Nijenborgh 4, NL-9747 AG Groningen, The Netherlands, Department of Physics, Uppsala University, Box 530, S-75121 Uppsala, Sweden, and Research Institute for Solid State Physics and Optics, Hungarian Academy of Sciences, P.O. Box 49, H-1525 Budapest, Hungary

Received: September 22, 2007; In Final Form: November 19, 2007

We demonstrate the growth of crystalline Li_4C_{60} films. The low-energy electron diffraction pattern of the films indicates the formation of polymer chains in the plane of the surface, consistent with the reported crystal structure. Electron energy loss and photoemission spectra identify the Li_4C_{60} polymer as a low band gap semiconductor, with a relatively strong coupling of electrons to low-frequency stretching modes of the polymer bonds and alkali phonons. No evidence is found for hybridization between the Li- and fullerene-derived electronic states. Instead, a partial charge transfer takes place, which is the same for different Li concentrations. This result rationalizes the stability of the polymer phase over a wide range of stoichiometries.

I. Introduction

In the solid state, C_{60} displays a remarkable tendency toward oligo- and polymerization, which is testified to by the number of phases characterized by covalent bonding between neighboring molecules.[1−14] Singly or doubly bonded dimers[1−4] and polymer chains,[5−8] as well as two-dimensional (2D)[9−11] and even three-dimensional[12−14] networks of C_{60} molecules have been reported. The free energy of different structures is often very similar, resulting in an abundance of phase transitions which can be induced by temperature or pressure variations, light irradiation, or chemical doping as in alkali fullerides.

In the case of 2D polymerization, different geometries and bonding motifs exist. Undoped C_{60} polymerizes either into a rhombohedral phase, characterized by hexagonal networks of molecules linked via [2 + 2]cycloaddition bonds which are coplanar with the hexagonal planes, or into a tetragonal phase, in which half the [2 + 2]cycloaddition bonds are coplanar with the networks while the others are orthogonal to them.[9,15] In Mg fullerides, the formation of a rhombohedral phase is reported,[16] while the 2D polymer phase of Na_4C_{60} consists of planar rectangular networks where each molecule forms four single bonds within the plane.[10] The rectangular polymer networks in Li-doped C_{60} were initially thought to consist of [2 + 2]-cycloaddition bonds.[17,18] However, more recent studies[19−21] have shown that the bonding motif is mixed, with [2 + 2]cycloaddition bonds in one direction and single bonds in the orthogonal direction.

Among alkali fullerides, 2D polymerization is only observed for the smallest alkali metals Li and Na. This is not the only peculiar feature of these compounds. While only few stable stoichiometries up to $x = 6$ are formed when C_{60} is intercalated with K, Rb, or Cs, a plethora of higher stoichiometries can be obtained with Na and Li. This is only partially due to the reduced radius of the intercalant, which allows multiple filling of the larger intercalation sites and diffusion into smaller interstices.[22] Stoichiometries up to $x = 28$ have been observed in Li-doped C_{60} with the formation of Li clusters in the largest interstitial voids between the fullerene molecules.[23] Such high alkali concentrations are clearly not compatible with a total charge transfer from the intercalant species. Some authors also suggest a partial covalency between the Li and fullerene electronic levels.[17,24,25]

For low Li concentrations $x \sim 1$, a tendency toward phase segregation was reported,[20,26] also observed in Na fullerides,[27] with the formation of alkali-poor regions and of a polymeric phase tentatively assigned an orthorhombic (one-dimensional (1D)) symmetry.[26] Photoemission studies on Li-doped C_{60} films with alkali concentration $x \leq 1$ have suggested the coexistence of two phases,[28,29] of which one would be a dimer phase analogous to that observed in the stoichiometric AC_{60} fullerides at low temperature (A = K, Rb, Cs). At intermediate Li concentrations, the aforementioned (monoclinic) 2D-polymer phase is present in the bulk at room temperature, which transforms into a metallic monomer phase at higher temperature.[20,30] In contrast with most alkali fullerides, where stable phases are obtained only for integer stoichiometry and the properties of, e.g., $x = 3$ or $x = 4$ phases are completely different, the 2D-polymer phase reported by Riccò et al.[20] is stable in the bulk over a broad range of (also noninteger) Li concentrations from $x = 3$ to $x = 5$.

To investigate the phase diagram of Li fullerides in thin-film form, we studied the intercalation of Li into C_{60} films by a combination of different electron spectroscopies. We demonstrate a simple protocol for the growth of polymeric Li_4C_{60} thin films by vacuum deposition and annealing and illustrate the fundamental properties of this phase.

II. Experiment

Experiments were conducted at the Zernike Institute for Advanced Materials of the University of Groningen, in an

* To whom correspondence should be addressed. E-mail: P.Rudolf@rug.nl.
[†] University of Groningen.
[‡] Uppsala University.
[§] Hungarian Academy of Sciences.

10.1021/jp077632t CCC: $40.75
Published on Web 02/05/2008

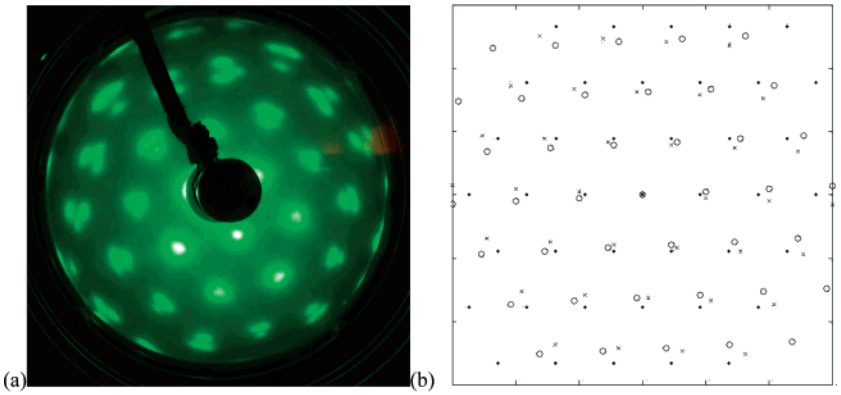

Figure 1. (a) LEED pattern of the polymer phase of a Li-doped film at primary electron energy of 35 eV, taken at room temperature after annealing to 370 K; note the grouping in triplets of spots. (b) Sketch of the pattern obtained by superposition of three distorted hexagonal patterns, each indicated with a different marker.

ultrahigh vacuum chamber equipped with low-energy electron diffraction (LEED), X-ray photoemission, and high-resolution electron energy loss spectroscopy (HREELS), and at the surface branch of beamline I-511 at the Swedish National Laboratory MAX-lab synchrotron facility in Lund.[31] In both cases, the films were grown in situ in a base pressure lower than 4×10^{-10} mbar and characterized at room temperature. Ordered C_{60} films were obtained by depositing C_{60} onto a metallic substrate in two steps, each followed by annealing, to form first an ordered monolayer and subsequently a multilayer film. Li intercalation was performed by sublimating Li from a thoroughly degassed commercial source (SAES Getters) onto a C_{60} multilayer. This was followed by annealing at different temperatures to check for phase formation.

In Groningen, the films were grown on a Ag single crystal oriented to within 0.5° of the (111) plane (Metal Crystals and Oxides), which was cleaned by cycles of argon ion bombardment (ion acceleration voltage 0.5 kV, ion emission current 15 mA) and annealing to 500 K. The temperature was monitored with a thermocouple attached next to the sample on the Mo sample holder. The crystallinity and purity of the substrate and of the pristine and doped C_{60} film were checked by LEED and X-ray photoemission. HREELS experiments were carried out with a commercial DELTA 0.5 spectrometer (SPECS). By varying the primary energy of the electron beam and the spectrometer resolution, we could investigate both the vibrational modes (in the meV energy-loss range) and the electronic transitions (eV range). The primary energy was set to 4 and 21 eV in the two cases, and the resolution on the Li-doped films (defined by the full-width-at-half-maximum of the elastic peak) was 3 meV and 0.01 eV, respectively. The spectra were measured in specular reflection geometry at an incidence angle of 55° and normalized to the intensity of the elastic peak.

High-resolution core level and valence-band photoemission (PES) spectra were acquired at beamline I-511 of MAX-lab on films grown on Au(111). This substrate had a hole on one side into which a thermocouple was inserted. The beamline end station[31] is equipped with a Scienta R4000 hemispherical electron energy analyzer, which can be rotated around the beam of the incoming linearly polarized light. This allows changing the angle of detection of the photoelectrons without modifying the geometry of the sample with respect to the photon beam, which impinges always with s-polarization at grazing incident (7° tilt angle) with respect to the substrate. PES spectra were acquired in two emission geometries, hereafter called "normal" (7° from the surface normal) and "grazing" (70°). Due to the finite electron mean free path in solids, a grazing emission spectrum is more surface-sensitive than a normal emission one, and the comparison between the two allows the determination of possible differences between the bulk and the surface of the film. The photon energy was 403 eV for the C 1s core level and 176 eV for the Li 1s and valence-band spectra. The photon energy resolution was 100 and 30 meV in the two cases. The analyzer resolution was set to 37.5 meV. The photon energies were chosen so that the photoelectron kinetic energies were the same for both core levels and similar for the C 1s and the valence band, so that the analyzer sensitivity and the inelastic mean free path (and hence the surface sensitivity) were the same for all spectra. All binding energies were referenced to the Fermi level of the clean Au substrate.

III. Results And Discussions

We start our discussion from LEED and HREELS results. Prior to Li intercalation, we verified by LEED that the surface of the C_{60}(111) multilayer grown on Ag(111) was hexagonal and monodomain (see ref 32 and references therein). While right after Li deposition at room temperature the average hexagonal symmetry was retained, upon annealing of the Li-doped films to 400 K a new LEED pattern arose with triple spots appearing at the positions of the pristine hexagonal lattice points, displayed in Figure 1a. The absence of the pristine spots (which should appear in the middle of each triplet) shows that this pattern is characteristic of a wholly different phase and that there are no extended domains of unreacted C_{60} in the film. The same LEED pattern was observed for different Li deposition times, which indicates that the same majority phase forms at different Li concentrations (see the discussion of the photoemission results).

Annealing to higher temperatures was found to sharpen the diffraction pattern, after which no further change was detected in subsequent anneals up to 575 K, the highest temperature reached during LEED experiments. The LEED pattern of the annealed Li_xC_{60} films consists of three distorted hexagonal patterns superposed upon one another, as visible in the scheme shown in Figure 1b. Such a LEED pattern indicates the presence of in-plane polymer chains in the surface layer of the film. These results are consistent with those of ref 26, where the formation of a polymeric phase was already observed after Li intercalation into a bulk C_{60} crystal at cryogenic temperature upon annealing the sample to the 320−370 K range.

In the presence of in-plane polymerization, the nearest neighbor inter-fullerene separation along the surface polymerization direction is shorter than that in the other directions, leading to a distorted-hexagonal (oblique) symmetry of the

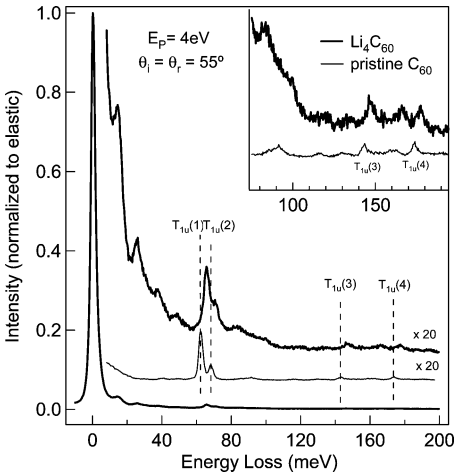

Figure 2. Comparison between the HREEL vibrational spectrum of polymeric Li_4C_{60} (bold line) and the analogous spectrum of the ordered C_{60} multilayer film (thin line). The dashed lines indicate the position of the four T_{1u} modes in the spectrum of the pristine C_{60} film.

surface plane. Since three possible surface polymerization directions exist (at 60° from each other), three equivalent domains appear in the LEED pattern, rotated by the same angle. We note that the LEED pattern in Figure 1a is inconsistent with a dimerization of the film, which would result in a doubling of the periodicity along one of the three surface directions.[33]

The LEED pattern of Figure 1a is instead consistent with the pattern expected for the termination plane of the 2D-polymer phase observed in bulk Li_xC_{60} ($3 < x < 5$).[19,20] The 2D polymeric networks in the monoclinic bulk phase form parallel to the (100) direction of the pristine fcc structure. Since the film termination of the pristine multilayer is (111), upon formation of the monoclinic phase in the film the 2D polymer networks are tilted with respect to the surface plane, with one bond direction parallel to the surface and the other lying at an angle of approximately 54.7° with respect to it. Three equivalent monoclinic domains are present, corresponding to the three possible polymerization directions in the hexagonal surface plane (once this direction is fixed, the other is uniquely determined). As the shortest intermolecular distance along the two polymerization directions is very similar, we cannot distinguish between the surface termination with in-plane [2 + 2]cycloaddition chains (corresponding to the (4,0,1) crystallographic plane in the structure identified in ref 20) and that with in-plane singly bonded chains (corresponding to the (0,4,1) termination). We also cannot exclude the presence of both types of termination.

Figure 2 shows the comparison between the HREEL vibrational spectrum of the undoped C_{60} multilayer and that of a typical Li_xC_{60} film. The vibrational features of the pristine C_{60} film are well-known (see ref 34 and references therein). The most striking difference between the two spectra is the enhancement of the loss intensity of the Li_xC_{60} spectrum in the frequency region corresponding to intermolecular vibrations and alkali-related modes (below ~30 meV). The loss intensity in the high-frequency region, where intramolecular vibrations occur, is instead comparable in the two systems.

Although the selection rules for HREELS in specular reflection geometry are the same as those for IR spectroscopy, HREELS is a surface-sensitive technique and the breaking of the inversion symmetry at the crystal's surface may modify the Raman and IR activity of surface modes. Moreover, so-called impact scattering processes, for which basically no selection rules apply, give a (weaker) contribution to the HREELS signal also in specular reflection. Hence, modes which are Raman-active in the bulk may be visible with HREELS.

In the Raman spectrum of the bulk polymer phase, three low-energy modes are observed, respectively at 16.5, 20, and 24.5 meV.[20] The energies of the first and third of these modes match well those of the two softest modes at 14 and 26 meV in the spectrum of Figure 2 (the bulk Raman-active mode at 20 meV might give rise to a less intense surface mode buried in the asymmetric tail of the feature at 14 meV). The modes visible in the HREEL spectrum of the Li-doped film at 38 and 48 meV correspond nicely to two intense Raman modes at 35 and 45 meV.[20] Small differences in the frequency of the modes can be expected between the bulk material and the film surface due to the different environment in the two cases.

The overall agreement between the HREEL spectrum of Figure 2 and the Raman spectrum of the 2D-polymer phase in the low-frequency range and the LEED evidence for polymer chains in the surface plane of our films are a clear indication that our growth method yields the same phase reported in ref 20 (see also below). We observed the same LEED pattern and phonon spectrum in films grown with the same method but with shorter or longer Li deposition times (i.e., for different nominal Li concentrations). This is in line with the reported stability of the bulk 2D-polymer phase over a wide stoichiometry range.[20] Following the authors of ref 20, in the remainder of the paper we will refer to this phase as Li_4C_{60} for brevity. Experimental stoichiometry estimates are given below for the films grown at MAX-lab.

Since the formation of polymer bonds reduces the symmetry of the fcc phase, the Li_4C_{60} modes can no longer be labeled with the representations derived from the icosahedral group. The point-group symmetry for the Li_4C_{60} polymer structure is C_{2h} ($C_2 \times i$). Group theory analysis shows that there are 174 distinct nondegenerate vibrational modes, all of which are either Raman- or IR-active in the bulk (Raman and IR modes are here mutually exclusive due to the presence of the inversion symmetry). The precise frequency of the HREEL modes of polymeric Li_4C_{60} depends on the bonding motif, on the degree of charge transfer to the fullerene network,[35,36] and on the modification of the crystal structure at the film surface. Due to the complexity of such analysis and the relatively low resolution of HREELS compared with Raman or IR, we do not attempt a rigorous assignment of all HREELS modes. Interesting information may, however, be obtained by comparison with the bulk studies on Li_4C_{60} and with other fullerides.

The intense low-energy modes visible in the HREEL spectrum of Li_4C_{60} are completely absent in the spectrum of the C_{60} multilayer film (see Figure 2), which shows that these soft modes arise from optical phonon modes involving the alkali atoms[37,38] and from vibrations of the polymeric intermolecular bonds.[39] A Raman-active mode related to a stretching vibration of the polymer bonds was observed at 14.6 meV in photopolymerized C_{60}.[40] This energy is close to that of the softest mode in the HREEL spectrum of Li_4C_{60} (16.5 meV).

Characteristic low-energy modes are also observed in the HREEL spectra of K_3C_{60} films[41] and of K-doped C_{60} monolayers for various alkali coverages.[37,38] In such systems the softest HREEL modes occur at an energy between 9 and 11 meV and are assigned to an alkali phonon.[37,38,41] Assuming that the energy of such alkali-related vibration scales with the inverse square root of the alkali mass (which is reasonable given the large mass of the fullerene molecule compared to that of the Li and K atoms), an analogous mode is expected in Li_4C_{60} at approximately 24 meV. This energy is very close to that of the

second feature (in the HREEL spectrum of Li_4C_{60} (at 26 meV)), which suggests an identification of this mode as a Li-related phonon.

The origin of the relatively high HREEL intensity of the softer modes and of the slow decaying slope of the elastic peak in the HREEL spectrum is not obvious. In fact, the observation of a sharp LEED pattern indicates that the tailing of the elastic peak is not due to disorder at the film surface. Also, a metallic origin of the slowly decaying tail is excluded, since (as shown below) the film is insulating. The relatively high intensity of the loss signal at lower frequencies in Li_4C_{60} might be related to a spectral enhancement due to the strong electron−phonon coupling between the soft phonons and electronic resonances, similar to what was observed in infrared reflection absorption spectra[42] and sum frequency generation spectra[43] of C_{60} films. Such a strong electron−phonon coupling to alkali phonons may be expected in polymeric Li_4C_{60} due to the presence of a semiconducting gap at the Fermi level (see below), which results in a poorer screening of alkali-related modes with respect to open-shell fullerides (see ref 44 and references therein).

Above 50 meV, the Raman spectrum shows many closely spaced peaks, which complicates the identification of the modes between 55 and 100 meV. Similar closely spaced lines were also observed in the Raman[36] and IR[45] spectra of a high-pressure high-temperature tetragonal C_{60} polymer, where intense modes are also visible at frequencies corresponding to the 38 and 48 meV modes. Densely spaced modes were also observed in the 50−100 meV energy range in the orthorhombic phase of pressure-polymerized C_{60} (both in Raman[46] and IR[47]) and in IR studies on orthorhombic RbC_{60} and CsC_{60}.[48,49] The point symmetry in these phases is D_{2h}, which contains more symmetry elements than the C_{2h} group of Li_4C_{60}.

Above 110 meV, the HREELS profile of the Li_4C_{60} film is very similar to that of the undoped multilayer (see Figure 2). The T_{1u} modes visible in the spectrum of the pristine multilayer film at 65, 71, 146, and 177 meV seem to give rise to somewhat broader features at roughly the same energies in the spectrum of the polymerized sample. The large width of the loss feature visible around 178 meV in the spectrum of the Li_4C_{60} film suggests that it arises from a combination of modes, probably derived from both the $T_{1u}(4)$ and the $A_g(2)$ modes. The latter cannot be resolved in our pristine spectrum but is reported at 178.4 meV in the HREEL spectrum of monolayer and multilayer (five molecular layers) C_{60} films.[37] Several polymer modes of tetragonal C_{60} are indeed found to derive from linear combinations of two, three, or more parent icosahedral modes.[45]

The closely related system Na_4C_{60} (C_i symmetry with space group $I2/m$)[10] has a lower point symmetry with respect to Li_4C_{60}, while maintaining the inversion symmetry. Also, in Na_4C_{60} all vibrational modes are nondegenerate. The similar stoichiometry and structure of these two fulleride phases suggests that their phonon spectrum should also be rather similar. Na_4C_{60} displays a series of strong IR features between 63 and 71 meV, of which the most intense is at 65 meV, and closely spaced peaks at 78.5, 83.2, 85.2, 88.5, and 90 meV. At higher frequency, two broad, intense features are visible at 98 and 146 meV, followed by a sharp peak at 176.4 meV.[50] The HREEL peaks visible at 66 and 71 meV in Li_4C_{60} have similar relative intensity and energy as the IR features of Na_4C_{60} in the range between 63 and 71 meV. The HREELS line shape between 79 and 90 meV in Li_4C_{60} is reminiscent of the IR features between 78.5 and 90 meV in Na_4C_{60}. The energy of the Li_4C_{60} peaks at 147 and 178 meV also fits nicely with that of the highest-frequency modes in Na_4C_{60}.

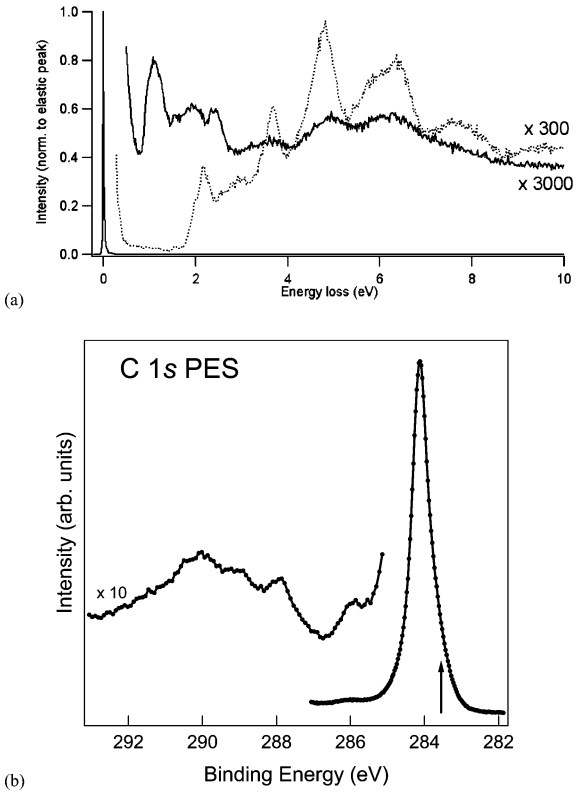

Figure 3. (a) HREELS spectrum of the electronic excitations of Li_4C_{60} (solid line), compared to that of the undoped C_{60} multilayer (dotted line). (b) C 1s photoemission spectrum of a typical Li_4C_{60} film. The shakeup region is also shown.

The mode at 98 meV in Na_4C_{60} corresponds to the Li_4C_{60} mode at 100 meV, both energies being very close to that of a characteristic mode in phases containing σ-bonded dimers,[51,52] which is usually taken as the signature of intermolecular bridging via single bonds. This further confirms our identification of the phase of our films as the same 2D-polymer phase identified in ref 20, rather than the orthorhombic phase, and might moreover indicate that the surface layer of the film contains in-plane single bonds.

With the use of diffraction theory, the average domain size of the films may be determined from the angular spread of the elastically scattered electron beam in the HREELS experiment. Assuming that the (surface) domains have the shape of round disks of typical diameter D, the full-width at half-maximum angular spread $\Delta\theta$ of the elastically scattered electrons in the (0,0) direction in reciprocal space is given[53] by the expression

$$2\Delta\theta \cos(\alpha) = \lambda/D$$

where λ is the de Broglie wavelength of the incoming electrons and α is the incidence angle with respect to the surface normal. Using the highly monochromatic electron beam at 4 eV, we found experimentally $\Delta\theta \sim 2°$ on the pristine C_{60} multilayer and $\Delta\theta \sim 3°$ for the Li_4C_{60} film. From these values a typical domain size D of 15 and 10 nm can be estimated for the pristine and Li-intercalated multilayer, respectively.

Figure 3a shows the high-energy (eV) losses of the same Li_4C_{60} film, together with the analogous spectrum of the pristine multilayer. The HREEL peaks in this energy range arise from electronic excitations in the film. The loss features above 3 eV in Li_4C_{60} (solid line) appear at the same energy as those of pristine C_{60} (dashed line), although they are much broader in the latter. A similar broadening (without significant shift in

energy) of the high-energy loss features was also observed in the HREEL spectrum of the orthorhombic (1D) polymer phase of CsC_{60},[54] which indicates that such features have a similar origin in all three systems. These higher energy loss features have been assigned to excitons, interband transitions, and a π plasmon which has an energy of about 6.3 eV.[34] The similarity in the high-energy line shape between the HREELS spectra of CsC_{60} and Li_4C_{60} and that of pristine C_{60} suggests that the electronic levels away from the Fermi energy E_F are not fundamentally altered by polymerization, as can be also recognized from our PES spectra (see discussion below).

A strong peak is visible at 1.1 eV in the Li_4C_{60} spectrum, with a shoulder around 0.8 eV energy loss. This peak, which lies in the fundamental gap of the undoped system, signals a strong reduction of the (band) gap in polymeric Li_4C_{60} with respect to pure C_{60}. No clear feature is observed in the Li_4C_{60} spectrum at 2.2 eV where the first intense loss occurs in pristine C_{60}. As can be seen from the normalization of the spectra, the lowest loss feature in C_{60} is much more intense than those observed in Li_4C_{60}. The absence of a corresponding feature in the Li_4C_{60} spectrum hence indicates that the percentage of unreacted C_{60} in the sample is very small if at all present, in line with our LEED results.

We can compare our HREEL spectrum to those measured on thin films of the monomeric A_4C_{60} compounds (A = K, Rb, Cs). The gap in these fullerides is on the order of 0.5−0.6 eV,[55−57] which is lower than the onset of the first loss feature in Li_4C_{60}. In the reflection HREELS spectrum of K_4C_{60}[58] and Cs_4C_{60},[59] the most intense feature occurs at 1.1 eV and is preceded by a broad bump or shoulder at 0.6 eV. Although the precise assignment of all intramolecular excitations is not yet known,[59] it has been argued that the spectral maxima between 1 and 2 eV in HREELS correspond to on-ball transitions, which have an onset around 1.1 eV,[55,58,59] and that the lower energy excitations correspond to transitions across the gap (such as the excitation from a Jahn−Teller split t_{1u} sublevel on one molecule to a higher-lying one on a neighboring fullerene[55]).

While the energy of the most intense electronic transition is the same (1.1 eV) in polymeric Li_4C_{60} and in monomeric A_4C_{60}, this does not occur for higher-energy excitations: two intense peaks are visible in the Li_4C_{60} spectrum at 2 and 2.4 eV, while the higher intramolecular excitations are observed at 1.36 and 1.65 eV in Cs_4C_{60}.[59] Moreover, no clear feature can be identified below 0.8 eV in the Li_4C_{60} spectrum. These differences clearly reflect the underlying differences between the monomer and 2D-polymer density of states (DOS) in the region close to the Fermi level, which will be discussed below. The comparison between Li_4C_{60} and the monomeric C_{60} and A_4C_{60} phases clearly shows that the HREELS features at 1.1, 2, and 2.4 eV in Li_4C_{60} are characteristic signatures of the lowest-energy electronic excitations in the polymer phase, which are distinct from those of monomer phases.

We now turn to our photoemission results. A rough stoichiometry estimate could be obtained for the films grown at MAX-lab from the ratio of the Li 1s to C 1s signal, normalized to the photon flux and to the relative cross section for photon absorption after subtraction of a Shirley background. Since the photoelectron kinetic energy was the same for both core levels, it was not necessary to correct the signal for the inelastic electron mean free path or analyzer throughput. For the stoichiometry determination, the intensity of the C 1s peak was divided by the number of carbon atoms in the fullerene cage (60). This procedure is expected to yield an overestimate of the true stoichiometry, as not all C atoms contribute the same intensity to the spectrum due to the attenuation of the photoemission signal across electron-rich regions. In particular, the C 1s signal stemming from the half-cages which lie below the intermolecular bonds with respect to the surface plane is lower than that arising in the upper half-cage. We indeed found that the nominal stoichiometry of our films was above 4.

Figure 3b shows the C 1s core level spectrum of a typical film. The main photoemission line in the C 1s spectrum is accompanied by an evident shakeup structure, similar to what is observed in pristine C_{60} (see ref 60 and references therein), with a first feature at 2 eV higher binding energy than the main line. This energy separation is close to the energy loss of the second and third features in HREELS. A direct comparison is, however, hindered by the intrinsic broadness of the spectral features in the shakeup spectrum and also because the creation of a core hole in the photoemission process leads to a different symmetry and energy of the shakeup states.[61] The observation of intense shakeup features points to a nonmetallic nature of our films, which is also confirmed by our valence-band PES data (see below).

The most interesting feature of the C 1s line is its asymmetry toward low binding energy (indicated by an arrow in Figure 3b). Upon polymerization, the C_{60} cages are distorted and charge density accumulates in the bond regions, leading to nonequivalent C sites near or far from the intermolecular bonds. The photoemission tail at low binding energy could then arise from the sp^3 orbitals of the C atoms directly involved in the intermolecular bonds. This is particularly interesting considering that similar effects have not been observed in a chemisorbed monolayer, where C_{60} is covalently bound to a metal surface,[32,54] nor in the photopolymer.[62,63] In covalent C_{60} monolayers on metals, the C 1s line width is smaller than that in metallic systems (see, e.g., refs 32 and 54), and the full-width-at-half-maximum of the C 1s line in photopolymerized C_{60} is only slightly larger[62,63] (by less than 0.1 eV) that that of pristine C_{60}. The difference with the Li_4C_{60} case, where two distinct C 1s lines are observed, could be related to the presence of the light Li counterions, which may occupy an off-centered position in the interstitial sites toward electron-rich regions in the polymer network (see discussion below).

The valence-band PES spectrum of the same Li_4C_{60} film is shown in Figure 4a. This spectrum is very similar to that of pristine C_{60}, though the peaks are broader and the valleys less marked. For convenience, we will refer to the peaks in the valence spectrum using the names of the C_{60} molecular orbitals, even though the electronic DOS of the polymer cannot be described in terms of the orbitals of the isolated C_{60} monomer, much as in the case of the vibrational modes.

The most evident change with respect to pristine C_{60} is the presence of two extra frontier states above the HOMO-like (HOMO = highest occupied molecular orbital) band, shown in more detail in the inset of Figure 4a. Such states, visible as two wide bumps of relatively low intensity centered at 1.2 and 0.5 eV binding energy, were already observed right after Li deposition. After a first annealing to 450 K, both became slightly sharper (not shown). Further annealing to 450−550 K did not modify the line shape, which indicates that a new stable phase of Li-doped C_{60} forms already just above room temperature, in agreement with our LEED study and in line with the results of ref 26. This shows, moreover, that no irreversible depolymerization occurs during the annealing (also to 550 K).

The photoemission intensity of the lowest binding energy feature decays smoothly toward the Fermi energy (E_F) where the spectral weight vanishes. The absence of intensity at E_F and

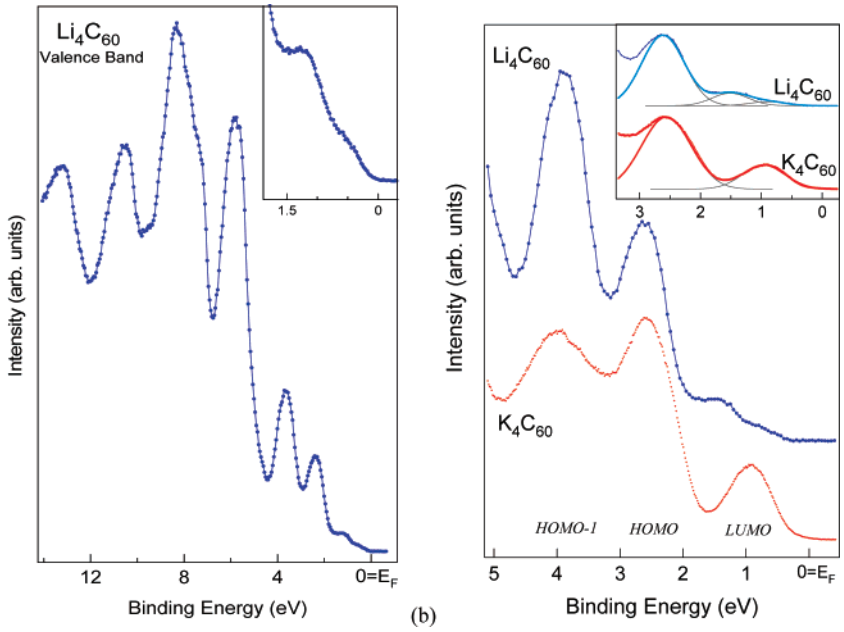

Figure 4. (a) Valence-band photoemission spectrum of polymeric Li_4C_{60}. The frontier states are shown in more detail in the inset. (b) Comparison between the HOMO-1, HOMO, and LUMO (LUMO = lowest unoccupied molecular orbital) region in K_4C_{60} and Li_4C_{60}. The inset shows the fit of the HOMO and LUMO region used for the estimation of charge transfer in Li_4C_{60}.

the small binding energy (0.5 eV) of the frontier feature demonstrates the nonconducting nature of the Li-doped film, while at the same time confirming the expectation for a small-gap semiconductor. It is interesting to note that apart from the features above of the HOMO-like states, the photoemission spectrum of polymeric Li_4C_{60} maintains a strong imprint of the molecular levels of the isolated C_{60} molecules. Also in other polymer structures the photoemission spectrum is found to match closely that of fcc C_{60},[62,63] contrary to phases containing C_{60} dimers where the modified symmetry of the molecular building unit determines a completely different DOS.[64] This similarity in the electronic structure far from E_F between monomer and polymer phases is consistent with the observed persistence of pure C_{60}-like features in the HREEL and C 1s shakeup spectra of Li_4C_{60} at high energy loss.

The two frontier states arise from the charge transfer from the Li atoms to the fullerene species. In monomer phases the LUMO-derived band lies, depending on the stoichiometry, at 1.6−1.8 eV lower binding energy than the HOMO-derived band (measured centroid-to-centroid).[65] This is also directly visible in the valence-band photoemission spectrum of K_4C_{60}, displayed in Figure 4b (own data from a separate experiment run, obtained at normal emission on a vacuum-distilled film with a photon energy of 90 eV). A smaller separation, of slightly more than 1 eV, is observed in Li_4C_{60} between the HOMO-like states and the higher binding energy frontier state. This confirms that the studied phase is not monomeric. Since no hybridization between Li and C states occurs and the contribution of Li signal in valence-band photoemission is too weak to significantly alter the photoemission line shape (see below), the spectrum of Figure 4a is indicative of the occurrence of polymerization, which determines a different electronic DOS with respect to that of the monomer phases.

The amount of charge transfer cannot be estimated with precision from the relative intensity of the valence-band features close to E_F, as such intensity is found experimentally to vary with the photon energy due to interference effects (see ref 66 and references therein). The relative intensity of the frontier states in Li_4C_{60} is, however, much smaller than the expectation for a charge transfer of four electrons per cage, which strongly suggests that only a partial charge transfer takes place in this system. In Figure 4b we compare the valence-band spectrum of our Li_4C_{60} film with that of K_4C_{60}, both normalized to the intensity of the HOMO-derived feature. The inset of Figure 4b shows a fit of the lowest binding energy features in the two compounds using Gaussian functions. The LUMO to HOMO intensity ratio in K_4C_{60}, calculated as the ratio of the areas of the corresponding Gaussian components, is found to be 0.3. Since the fullerene HOMO is 5-fold degenerate, the expected ratio as determined by the relative electron occupancies of the two orbitals in K_4C_{60} is 4:10 or 0.4 (complete charge transfer occurs[67] in K_4C_{60}). The small deviation from the nominal ratio in K_4C_{60} can be ascribed to the aforementioned fluctuations of the relative intensities of the PES features. In Li_4C_{60} the corresponding ratio is only 0.2, which would correspond to a charge transfer of only 2 electrons per cage to the fullerene network. Even taking K_4C_{60} as our reference for a charge transfer of 4 electrons per cage, the charge transfer in Li_4C_{60} would still be at the most 2/3 of this value, namely, 2.67 electrons per cage. This last value can be taken as an upper limit for the actual amount of charge transfer in Li_4C_{60}, as the charge transfer estimate obtained from the relative intensity of, e.g., the LUMO and HOMO-1 features of Li_4C_{60} is even lower than 2, as can be seen directly from the comparison with K_4C_{60} in Figure 4b (the same holds also if another higher binding energy orbital is taken for the comparison).

A partial charge transfer of only 2 or 2.5 electrons per cage can actually be expected for the present system. In the Li_xCsC_{60} family and in Li_2RbC_{60}, for example, the Li atoms only transfer a fraction equal to roughly 70% of their Li 2s electrons to the fullerene species.[68] Unlike the case of Na fullerides where charge transfer is believed to be complete up to a doping level of $x \leq 6$,[69] partial electron transfer already occurs at lower doping levels in Li fullerides. The neutral atomic radius of Li is comparable to the ionic radius of K and Rb and smaller than the ionic radius of Cs. Hence nonionized or partially ionized Li atoms can intercalate not only into the large octahedral sites of the pristine fcc structure but also into the smaller tetrahedral ones.

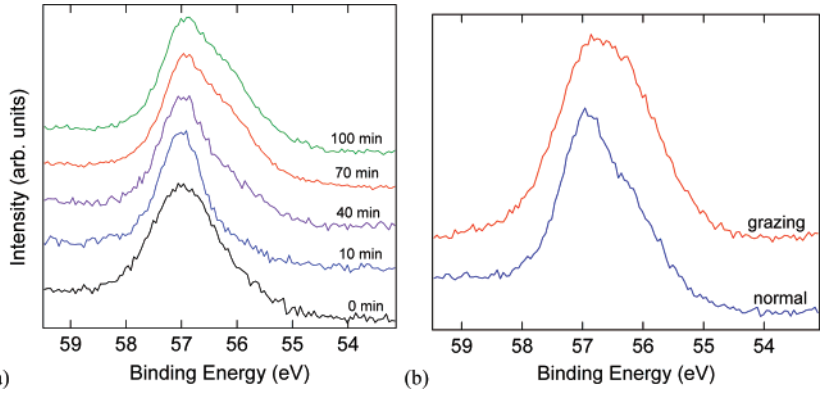

Figure 5. (a) Dependence of the Li 1s photoemission spectrum upon annealing at 450 K, for different annealing times. (b) Angular dependence of the Li 1s photoemission spectrum of a Li_4C_{60} film in its most stable configuration (see text). All spectra are normalized to the intensity maximum.

Moreover, a charge transfer of 2 or 2.5 electrons is consistent with the observation of the polymer phase already at a doping level of $x = 3$ in the bulk. Such a charge transfer is sufficient to stabilize the formation of the Li_4C_{60} polymer network. In fact, while a charge transfer is usually necessary to stabilize the bridging of two adjacent molecules via a single bond, which uses up one electron per participating cage,[70] [2 + 2]cycloaddition bonding between neighboring C_{60} molecules is observed in all polymer phases derived from undoped C_{60} (where no charge transfer is present).[9,40,71,72] Since each cage is linked by two [2 + 2]cycloaddition bonds and two single bonds, a doping level of two electrons per cage is sufficient for the formation of the 2D-polymer phase in Li_4C_{60}.

Since no hybridization is present between the Li- and C_{60}-derived levels,[20,29] a partial electron transfer entails that some charge density remains in the Li 2s orbitals, either at Li atoms located close to the fullerene network or at Li clusters occupying pseudo-octahedral sites as in the higher Li stoichiometries such as $Li_{12}C_{60}$ and $Li_{15}C_{60}$ or both (see the discussion of the Li 1s spectrum below). The contribution of Li 2s states to the valence-band spectrum, which would provide a direct proof of incomplete charge transfer, cannot be detected due to the much lower photoionization cross section[73,74] of the Li 2s orbital (by at least a factor of 10) with respect to carbon valence states over the whole photon energy range available on beamline I511.[31]

The valence-band spectrum of our Li_4C_{60} films is very similar to that obtained by Schnadt et al. on a Li-doped film of average stoichiometry $x \leq 1$.[29] In particular, the shape, relative intensity and binding energy of the two frontier features are practically identical. These authors measured the valence-band spectrum immediately after Li intercalation at room temperature and found that annealing to 375 K did not significantly alter the spectrum. The close resemblance of the spectra, the identical sample preparation, and the fact that we also observe the formation of a stable phase already upon Li deposition show that the phase observed in ref 29 is in fact the same Li_4C_{60} polymer phase reported here. Indeed, while these authors tentatively assign the double feature above the HOMO to the presence of two phases in their film and assume that one of these phases consists of C_{60} dimers as the metastable phase of AC_{60} compounds (A = K, Rb, Cs), there is no evidence in bulk studies for the formation of a dimer structure at low Li stoichiometry,[20,26] and our LEED study excludes the presence of dimer domains at the film surface.

We argue instead that the states below 2 eV binding energy in the valence-band spectra of our film and of ref 29 are characteristic of the Li_4C_{60} polymer phase. No theoretical DOS has appeared for the Li_4C_{60} phase, but calculations exist for the 2D-tetragonal networks of tetragonal C_{60} (where, however, as discussed in the Introduction, the bonding motif is different than that in monoclinic Li_4C_{60}). The C_{60} tetragonal polymer is insulating with a fundamental gap of the order of 1.2 eV and a second gap in the DOS 2 eV above the HOMO-like band (see, e.g., Figure 6(a) of ref 72). The energy separation between the HOMO-like states and the two frontier features in Li_4C_{60} (see Figure 4) compare rather well to these values, which suggests that the electronic DOS in Li_4C_{60} is not so dissimilar from that of the neutral tetragonal polymer. Hence, it is not totally unexpected that the valence-band spectrum of Li_4C_{60} is structured in the frontier region just below E_F. The highest occupied state in the spectrum of Li_4C_{60} phase could correspond to a nondegenerate "LUMO-like" frontier orbital, as in the case of tetragonal C_{60} where the effective degeneracy of the unoccupied frontier states is lifted upon polymerization.[75] A charge transfer from the Li atoms of two electrons per cage would result in the total filling of such a frontier state, leading to an electronic structure characterized by a band gap. This might be at the origin of the insulating nature of the Li_4C_{60} phase. The presence of two distinct features in the frontier states of Li_4C_{60} is in line with the rich structure observed in the HREEL spectrum of this phase, which indicates the existence of several possible interband electronic transitions between occupied and empty valence-band states.

Figure 5a displays the variation of the normal emission Li 1s signal as a function of annealing time at 450 K. The Li 1s peak is the only spectroscopic feature which exhibits a clear dependence on thermal treatment. The spectrum taken right after Li intercalation ($t = 0$ min) consists of a broad, structureless feature. After the first anneal ($t = 10$ min), the Li 1s peak became sharper, indicating that order in the film had improved. This spectrum looks identical to that measured in ref 29. Upon further annealing, a second Li 1s component appeared at lower binding energy. As seen in Figure 5a, the relative intensity of this component increased upon annealing until it was saturated at approximately half the intensity of the higher binding energy component. Further annealing (up to 550 K, not shown) did not result in any further change of the Li 1s signal. The Li 1s spectrum corresponding to this film configuration is shown in Figure 5b, in both normal and grazing emission geometry. In both emission geometries, two components are visible, approximately 0.8 eV apart. The two components have comparable intensity in grazing emission, while as already mentioned the component at higher binding energy is more intense in normal emission.

The presence of two nonequivalent Li components might in principle reflect the existence of different Li oxidation states in

the film. However, the observed changes in the relative intensity of the two Li components upon annealing (see Figure 5a) are not accompanied by changes in the valence band reflecting a lower or higher amount of charge transfer. Instead, it was shown in ref 20 that two types of Li intercalation sites exist in the 2D polymeric structure of Li_4C_{60}, which can be thought to derive from the interstitial sites of the fcc structure via the polymerization-induced distortion of the lattice. Per fullerene cage, there are two pseudo-tetrahedral sites and one pseudo-octahedral site (for a total of three sites). Of the four Li atoms per cage in stoichiometric Li_4C_{60}, supposedly two share the largest pseudo-octahedral void, and the other two each occupy a pseudo-tetrahedral void.[20] The binding energy difference observed in the Li 1s spectra of Figure 5 is close to that expected between octahedral and tetrahedral intercalants in monomer phases. We associate the higher binding energy component with the octahedral sites, in analogy with other alkali fullerides. A single Li 1s component is also observed in films with low Li concentration.[29] The initial presence in our spectra of only the higher binding energy component indicates that after the first annealing only pseudo-octahedral sites are occupied and all Li ions have the same (noninteger) charge state.

For all films the Li concentration as determined from PES data was higher in grazing emission than in normal emission, indicating either a Li termination of the films (which could explain the relative instability of the films over time) or a higher Li content at the film surface with respect to subsurface layers. The variation in shape of the Li 1s signal upon annealing and between the two emission geometries suggests that the occupancy of the two types of sites is a function of temperature or thermal treatment and possibly of the distance from the film surface.

The lack of dependence of the valence-band states upon annealing suggests that partial charge transfer occurs from both types of sites. This is possibly related to a displacement of Li ions toward electron-rich sites in the fullerene polymer network. Such a displacement and the resulting nonequivalence of the Madelung potential at different C sites might also be responsible for the clear observation of distinct lines in the C 1s spectrum.

Especially in films annealed to below 475 K, the Li atoms displayed a tendency to slowly migrate to the film surface, testified to by an increase and broadening of the Li 1s signal over a time period of several hours with the sample at room temperature (not shown). Upon subsequent annealing at 450 K or higher, the initial surface stoichiometry could be recovered and the Li 1s feature assumed the line shape corresponding to the spectrum shown in Figure 5b. The observation of Li diffusion in the polymer matrix is inconsistent with hybridization between Li- and C-derived levels, as already pointed out in ref 20. The lack of hybridization is in line with the largely ionic bonding observed[29] in films with nominal stoichiometry of $x \leq 1$. The fact that despite the variation in shape and intensity of the Li 1s signal in time that virtually no change occurs in the valence-band frontier states clearly points to the existence of a charge transfer saturation threshold in Li_4C_{60}. The existence of such threshold, besides confirming the partial character of the charge transfer, explains the observed bulk stability[20] of the polymer phase over a wide range of Li stoichiometries.

IV. Conclusions

We demonstrated the growth of polymeric Li_4C_{60} in thin-film form. The Li_4C_{60} phase is formed already by Li deposition on a C_{60} multilayer at room temperature, while annealing to above 400 K is found to enhance ordering in the film. The LEED pattern indicates the presence of polymer chains in the surface layer, which corresponds to either the (4,0,1) or (0,4,1) termination plane of the bulk crystal. Electron-energy loss and photoemission data provide evidence that this phase is a low band gap semiconducting polymer with a relatively strong electron−phonon coupling to the soft alkali-related and intermolecular modes. In the valence-band photoemission spectrum, two frontier spectral features characteristic of the polymer phase are observed above the HOMO-like feature at 1.2 and 0.5 eV binding energy. The lack of dependence of such features on the relative Li concentration excludes the possibility of Li−C hybridization, while it demonstrates the existence of a charge transfer saturation threshold from the Li atoms to the fullerene network, corresponding to an only partial transfer of 2−2.5 electrons per cage. This rationalizes the reported stability of the polymer phase over a wide stoichiometry range.

Acknowledgment. The authors thank Franz Hennies for critical reading of the manuscript. This work was performed within the pilot project of coordinated collaborative research training at the Ångström Laboratory of Uppsala University and at the Zernike Institute for Advanced Materials of the University of Groningen and received additional financial support from the Dutch Foundation for Fundamental Research on Matter (FOM) and the Breedtestrategie program of the University of Groningen and from the Stiftelsen för Strategisk Forskning and the Vetenskapsrådet. Valuable support from Franz Hennies and the MAX-lab staff is gratefully acknowledged.

References and Notes

(1) Oszlányi, G.; Bortel, G.; Faigel, G.; Tegze, M.; Gránásy, L.; Peckker, S.; Stephens, P. W.; Bendele, G.; Dinnebier, R.; Mihály, G.; Jánossy, A.; Chauvet, O.; Forró, L. *Phys. Rev. B: Condens. Matter Mater. Phys.* **1995**, *51*, 12228−12232.

(2) Zhu, Q.; Cox, D.; Fischer, J. E. *Phys. Rev. B: Condens. Matter Mater. Phys.* **1995**, *51*, 3966−3969.

(3) Thier, K.-F.; Mehring, M.; Rachdi, F. *Phys. Rev. B: Condens. Matter Mater. Phys.* **1997**, *55*, 124−126.

(4) Wang, G.-W.; Komatsu K.; Murata Y.; Shiro M. *Nature* **1997**, *387*, 583−586.

(5) Stephens, P. W.; Bortel, G.; Faigel, G.; Tegze, M.; Jánossy, A.; Peckker, S.; Oszlányi, G.; Forró, L. *Nature* **1994**, *370*, 636−639.

(6) Chauvet, O.; Oszlányi, G.; Forró, L.; Stephens, P. W.; Tegze, M.; Faigel, G.; Jánossy, A. *Phys. Rev. Lett.* **1994**, *72*, 2721−2724.

(7) Pekker, S.; Forró, L.; Mihály, G.; Jánossy, A. *Solid State Commun.* **1994**, *90*, 349−352.

(8) Bendele, G. M.; Stephens, P. W.; Prassides, K.; Vavekis, K.; Kordatos, K.; Tanigaki, K. *Phys. Rev. Lett.* **1998**, *80*, 736−739.

(9) Nuñez-Regueiro, M.; Marques, L.; Hodeau, J.-L.; Béthoux O.; Perroux M. *Phys. Rev. Lett.* **1995**, *74*, 278−281.

(10) Oszlanyi, G.; Baumgartner, G.; Faigel, G.; Forró, L. *Phys. Rev. Lett.* **1997**, *78*, 4438−4441.

(11) Okotrub, A. V.; Belavin, V. V.; Bulusheva, L. G.; Davydov, V. A.; Makarova, T. L.; Tománek, D. *J. Chem. Phys.* **2001**, *115*, 5637−5641.

(12) Blank, V. D.; Buga, S. G.; Dubitsky, G. A.; Serebryanaya, N. R.; Popov, M. Y.; Sundqvist, B. *Carbon* **1998**, *36*, 319−343.

(13) Marques, L.; Mezouar, M.; Hodeau, J.-L.; Nunez-Regueiro M.; Serebryanaya N. R.; Ivdenko V. A.; Blank, V. D.; Dubitsky, G. A. *Science* **1999**, *283*, 1720−1723.

(14) Yamanaka, S.; Kubo, A.; Inumaru, K.; Komaguchi, K.; Kini, N. S.; Inoue, T.; Irifune, T. *Phys. Rev. Lett.* **2006**, *96*, 076602.

(15) Davydov, V. A.; Kashevarova, L. S.; Rakhmanina, A. V.; Agafonov, V.; Allouchi, H.; Ceolin, R. A.; Dzyabchenko, V.; Senyavin, V. M.; Szwarc, H. *Phys. Rev.* **1998**, *58*, 14786−14790.

(16) Borondics, F.; Oszlanyi, G.; Faigel, G.; Pekker, S. *Solid State Commun.* **2003**, *127*, 311−313.

(17) Yasukawa, M.; Yamanaka, S. *Chem. Phys. Lett.* **2001**, *341*, 467−475.

(18) Wagberg, T.; Stenmark, P.; Sundqvist, B. *J. Phys. Chem. Solids* **2004**, *65*, 317−320.

(19) Margadonna, S.; Pontiroli, D.; Belli, M.; Shiroka, T.; Riccò, M.; Brunelli, M. *J. Am. Chem. Soc.* **2004**, *126*, 15032−15033.

(20) Riccò, M.; Shiroka, T.; Belli, M.; Pontiroli, D.; Pagliari, M.; Ruani, G.; Palles, D.; Margadonna, S.; Tomaselli, M. *Phys. Rev. B: Condens. Matter Mater. Phys.* **2005**, *72*, 155437.

(21) Wagberg, T.; Johnels, D. *J. Phys. Chem. Solids* **2006**, *67*, 1091−1094

(22) Dresselhaus, M. S.; Dresselhaus, G.; Eklund, P. C. *Science of Fullerenes and Carbon Nanotubes*; Academic Press: San Diego, CA, 1996.

(23) Cristofolini, L.; Riccò, M.; De Renzi, R. *Phys. Rev. B: Condens. Matter Mater. Phys.* **1999**, *59*, 8343−8346.

(24) Hamamoto, N.; Jitsukawa, J.; Sakoto, C. *Eur. Phys. J. D* **2002**, *19*, 211−221.

(25) Hirosawa, I.; Prassides, K.; Mizuki, J.; Tanigaki, K.; Gevaert, M.; Lappas, A.; Cockcroft, J. K. *Science* **1994**, *264*, 1294−1297.

(26) Dilanyan, R. A.; Khasanov, S. S.; Bredikhin, S. I.; Gurov, A. F.; Kveder, V. V.; Osip'yan, Yu. A.; Shalynin, A. I. *JETP* **2001**, *93*, 1239−1244.

(27) Klupp, G.; Matus, P.; Quintavalle, D.; Kiss, L. F.; Kováts, É.; Nemes, N. M.; Kamarás, K.; Pekker, S.; Jánossy, A. *Phys. Rev. B: Condens. Matter Mater. Phys.* **2006**, *74*, 195402.

(28) Gu, C.; Poirier, D. M.; Jost, M. B.; Benning, P. J.; Chen, Y.; Ohno, T. R.; Martins, J. L.; Weaver, J. H. *Phys. Rev. B: Condens. Matter Mater. Phys.* **1992**, *45*, 6348−6351.

(29) Schnadt, J.; Brühwiler, P. A.; Mårtensson, N.; Lassesson, A.; Rohmund, F.; Campbell, E. E. B. *Phys. Rev. B: Condens. Matter Mater. Phys.* **2000**, *62*, 4253−4256.

(30) Riccò, M.; Belli, M.; Pontiroli, D.; Mazzani, M.; Shiroka, T.; D. Arčon, D.; Zorko, A.; Margadonna, S.; Ruani, G. *Phys. Rev. B: Condens. Matter Mater. Phys.* **2007**, *75*, 081401(R).

(31) Denecke, R.; Väterlein, P.; Bässler, M.; Wassdahl, N.; Butorin, S.; Nilsson, A.; Rubensson, J.-E.; Nordgren, J.; Mårtensson, N.; Nyholm, R. *J. Electron Spectrosc. Relat. Phenom.* **1999**, *101*−*103*, 971−977.

(32) Rudolf, P. In *Electronic Properties of Novel Materials: Fullerenes and Fullerene Nanostructures*; Kuzmany, H., Fink, J., Mehring, M., Roth, S. Eds.; World Scientific Publishing Co., Ltd.: Singapore, 1996; pp 263−275.

(33) This is true both if the dimers form parallel to the surface and in the case where they are tilted with respect to the surface hexagonal layer.

(34) Lucas, A.; Gensterblum, G.; Pireaux, J. J.; Thiry, P. A.; Caudano, R.; Vigneron, J. P.; Lambin, Ph.; Krätschmer, W. *Phys. Rev. B: Condens. Matter Mater. Phys.* **1992**, *45*, 13694−13702.

(35) Rao, A. M.; Eklund, P. C.; Hodeau, J.-L.; Marques, L.; Nunez-Regueiro, M. *Phys. Rev. B: Condens. Matter Mater. Phys.* **1997**, *55*, 4766−4773.

(36) Davydov, V. A.; Kashevarova, L. S.; Rakhmanina, A. V.; Senyavin, V. M.; Céolin, R.; Szwarc, H.; Allouchi, H.; Agafonov, V. *Phys. Rev. B: Condens. Matter Mater. Phys.* **2000**, *61*, 11936−11945.

(37) Silien, C.; Caudano, Y.; Peremans, A.; Thiry P. A. *Appl. Surf. Sci.* **2000**, 162−163, 445−451.

(38) Silien, C.; Thiry, P. A.; Caudano, Y. *Surf. Sci.* **2004**, *558*, 174−180.

(39) Porezag, D.; Pederson, M. R.; Frauenheim, Th.; Köhler, Th. *Phys. Rev. B: Condens. Matter Mater. Phys.* **1995**, *52*, 14963−14970.

(40) Rao, A. M.; Zhou, P.; Wang, K. A.; Hager, G. T.; Holden, J. M.; Wang, Y.; Lee, W. T.; Bi, X. X.; Eklund, P. C.; Cornett, D. S.; Duncan, M. A.; Amster, I. J. *Science* **1993**, *259*, 955−957.

(41) Silien, C.; Thiry, P. A.; Caudano, Y. *Appl. Surf. Sci.* **2004**, *237*, 477−481.

(42) Rudolf, P.; Raval, R.; Dumas, P.; Williams, G. P. *Appl. Phys. A: Mater. Sci. Process.* **2002**, *75*, 147−153.

(43) Humbert, C.; Caudano, Y.; Dreesen, L.; Sartenaer, Y.; Mani, A. A.; Silien, C.; Lemaire, J.-J.; Thiry, P. A.; Peremans, A. *Appl. Surf. Sci.* **2004**, *237*, 463−469.

(44) Wehrli, S.; Rice, T. M.; Sigrist, M. *Phys. Rev. B: Condens. Matter Mater. Phys.* **2004**, *70*, 233412.

(45) Zhu, Z.-T.; Musfeldt, J. L.; Kamarás, K.; Adams, G. B.; Page, J. B.; Kashevarova, L. S.; Rakhmanina, A. V.; Davydov, V. A. *Phys. Rev. B: Condens. Matter Mater. Phys.* **2002**, *65*, 085413.

(46) Persson, P.-A.; Edlund, U.; Jacobsson, P.; Johnels, D.; Soldatov, A.; Sundqvist, B. *Chem. Phys. Lett.* **1996**, *258*, 540−546.

(47) Long, V. C.; Musfeldt, J. L.; Kamarás, K.; Adams, G. B.; Page, J. B.; Iwasa, Y.; Mayo, W. E. *Phys. Rev. B: Condens. Matter Mater. Phys.* **2000**, *61*, 13191−13201.

(48) Kamarás, K.; Iwasa, Y.; Forró, L. *Phys. Rev. B: Condens. Matter Mater. Phys.* **1997**, *55*, 10999−11002.

(49) Kamarás, K.; Pekker, S.; Forró, L.; Tanner, D. B. *Chem. Phys. Lett.* **1998**, *295*, 279−284.

(50) Klupp, G.; Borondics, F.; Oszlányi, G.; Kamarás, K. Distortions of C_{60}^{4-} studied by infrared spectroscopy. In *Proceedings of the XVIIth International Winterschool on Electronic Properties of Novel Materials*, Kirchberg, Austria, March 8−15, 2003; Kuzmany, H., et al., Eds.; AIP Conference Proceedings, 2003; Vol. 685, pp 62−65.

(51) Kamarás, K.; Tanner, D. B.; Forró, L. *Fullerene Sci. Tech.* **1997**, *5*, 465−478.

(52) Kürti, J.; Borondics, F.; Klupp, G. *AIP Conf. Proc.* **2001**, *591*, 25.

(53) Ertl, G.; Kuppers, I. *Low Energy Electrons and Surface Chemistry*; Verlag Chemie: Berlin, 1974.

(54) Rudolf, P.; Golden, M. S.; Brühwiler, P. A. *J. Electron Spectrosc. Relat. Phenom.* **1999**, *100*, 409−433.

(55) Knupfer, M.; Fink, J. *Phys. Rev. Lett.* **1997**, *79*, 2714−2717.

(56) Chibotaru, L. F.; Ceulemans, A.; Cojocaru, S. P. *Phys. Rev. B: Condens. Matter Mater. Phys.* **1999**, *59*, R12728−12731.

(57) Golden, M. S.; Knupfer, M.; Fink, J.; Armbruster, J. F.; Cummins, T. R.; Romberg, H. A.; Roth, M.; Sing, M.; Schmidt, M.; Sohmen, E. *J. Phys.: Condens. Matter* **1995**, *7*, 8219−8247.

(58) Lopinski, G. P.; Mitch, M. G.; Chase, S. J.; Lannin, J. S. In *Science and Technology of Fullerene Materials*; Bernier, P., Ebbesen, T. W., Bethuri, V. S., Metzger, R. M., Chiang, L. Y., Mintmire, J. W., Eds.; MRS Symposia Proceedings No. 359; Materials Research Society: Pittsburgh, PA, 1995; p 301.

(59) Hunt, M. R. C.; Rudolf, P.; Modesti, S. *Phys. Rev. B: Condens. Matter Mater. Phys.* **1997**, *55*, 7889−7903.

(60) Enkvist, C.; Lunell, S.; Sjögren, B.; Svensson, S.; Brühwiler, P. A.; Nilsson, A.; Maxwell, A. J.; Mårtensson, N. *Phys. Rev. B: Condens. Matter Mater. Phys.* **1993**, *48*, 14629−14637.

(61) Schnadt, J.; Schiessling, J.; Brühwiler, P. A. *Chem. Phys.* **2005**, *312*, 39−45.

(62) Onoe, J.; Nakao, A.; Takeuchi, K. *Phys. Rev. B: Condens. Matter Mater. Phys.* **1997**, *55*, 10051−10056.

(63) Itchkawitz, B. S.; Long, J. P.; Schedel-Niedrig, T.; Kabler, M. N.; Bradshaw, A. M.; Schlögl, R.; Hunter, W. R. *Chem. Phys. Lett.* **1995**, *243*, 211−216.

(64) Pichler, T.; Knupfer, M.; Golden, M. S.; Haffner, S.; Friedlein, R.; Fink, J.; Andreoni, W.; Curioni, A.; Keshavarez-K, M.; Bellavia-Lund, C.; Sastre, A.; Hummelen, J. C.; Wudl, F. *Phys. Rev. Lett.* **1997**, *78*, 4249−4252.

(65) Macovez, R.; Rudolf, P.; Marenne, I.; Kjeldgaard, L.; Brühwiler, P. A.; Pichler, T.; Vilmercati, P.; Larciprete, R.; Petaccia, L.; Bertoni, G.; Goldoni, A. *Phys. Rev. B: Condens. Matter Mater. Phys.* **2007**, *75*, 195424.

(66) Hunt, M. R. C.; Pichler, T.; Šiller, L.; Brühwiler, P. A.; Golden, M. S.; Tagmatarchis, N.; Prassides, K.; Rudolf, P. *Phys. Rev. B: Condens. Matter Mater. Phys.* **2002**, *66*, 193404.

(67) Molodtsov, S. L.; Gutierrez, A.; Navas, E.; Domke, M.; Kaindl, G.; Merkel, M.; Nucker, N.; Fink, J.; Antropov, V. P.; Andersen, O. K.; Jepsen, O. *Z. Phys. B* **1993**, *92*, 347−351.

(68) Kosaka, M.; Tanigaki, K.; Prassides, K.; Margadonna, S.; Lappas, A.; Brown, C. M.; Fitch, A. N. *Phys. Rev. B: Condens. Matter Mater. Phys.* **1999**, *59*, R6628−R6630.

(69) Andreoni, W.; Giannozzi, P.; Armbruster, J. F.; Knupfer, M.; Fink, J. *Europhys. Lett.* **1996**, *34*, 699−704.

(70) Pekker, S.; Oszlányi, G.; Faigel, G. *Chem. Phys. Lett.* **1998**, *282*, 435−441.

(71) Xu, C. H.; Scuseria, G. E. *Phys. Rev. Lett.* **1995**, *74*, 274−277.

(72) Okada, S.; Saito, S. *Phys. Rev. B: Condens. Matter Mater. Phys.* **1999**, *59*, 1930−1936.

(73) Yeh J. J. *Atomic Calculation of Photoionization Cross-Sections and Asymmetry Parameters*; Gordon and Breach Science Publishers: Langhorne, PA, 1993.

(74) Yeh, J. J.; Lindau, I. *Atomic Data and Nuclear Data Tables* **1985**, *32*, 1−155.

(75) Belavin, V. V.; Bulusheva, L. G.; Okotrub, A. V.; Tomanek, D. *J. Phys. Chem. Solids* **2000**, *61*, 1901−1911.